



The University of Sydney

School of Civil Engineering
Sydney NSW 2006
AUSTRALIA

<http://www.civil.usyd.edu.au/>

Centre for Advanced Structural Engineering

**The behaviour of drive-in racks under
horizontal impact load**

Research Report No R871

Vinh Hua, BE

Kim JR Rasmussen, MScEng, PhD

July 2006

ISSN 1833-2781



The University of Sydney

School of Civil Engineering
Centre for Advanced Structural Engineering
<http://www.civil.usyd.edu.au/>

The behaviour of drive-in racks under horizontal impact load

Research Report No R871

Vinh Hua, BE
Kim Rasmussen, MScEng, PhD

July 2006

Abstract:

This report is concerned with the behaviour of drive-in steel storage racks under horizontal impact load in the down-aisle direction. Such impact loads due to forklifts striking an upright is a major cause of structural failure for drive-in rack systems.

The report investigates the load path through the rack structure by the use of finite element analysis. A series of parametric studies is carried out to study the influence of the number of bays in the down-aisle direction on the behaviour of the system. A simplified design model is also developed and compared with finite element predictions of displacements and internal forces, generally showing good agreement.

Keywords:

Drive-in racks, steel storage racks, steel structures, finite element analysis, design.

Copyright Notice

School of Civil Engineering, Research Report R871

The behaviour of drive-in racks under horizontal impact load

© 2006 Vinh Hua and Kim JR Rasmussen

K.Rasmussen@civil.usyd.edu.au

This publication may be redistributed freely in its entirety and in its original form without the consent of the copyright owner.

Use of material contained in this publication in any other published works must be appropriately referenced, and, if necessary, permission sought from the author.

Published by:
School of Civil Engineering
The University of Sydney
Sydney NSW 2006
AUSTRALIA

July 2006

This report and other Research Reports published by The School of Civil Engineering are available on the Internet:

<http://www.civil.usyd.edu.au>

Table of Contents

Table of Contents	3
1 Introduction	4
2 Methodology	4
3 Finite element model	5
3.1 Geometry and Element Types	5
3.2 Materials	5
3.3 Loading	5
4 Analysis results	5
4.1 Load path	5
4.2 Sensitivity study results	6
5 Mechanical model	7
5.1 Development of model	7
5.2 Worked example	10
6 Conclusions	11
7 References	12
Appendix A: Notation	13
Appendix B: Derivation of spine bracing distortion	14
Appendix C: Derivation of stiffness of uprights in the down-aisle direction allowing for semi-rigid joints at the base and at the upright-portal beam connection	16
Tables	18
Figures	19
Figure 1. Selective and drive-in rack systems	19
Figure 2. Drive-in Rack Arrangement	20
Figure 3. 3D View of Drive-in Rack Model	21
Figure 4. Standard Siemens Upright RF11024	21
Figure 5. Standard Siemens Sigma Beam SB9016	22
Figure 6. Standard Siemens Pallet Runner	22
Figure 7a. Load path through front row of drive-in rack	23
Figure 7b. Load path through top plan bracing	23
Figure 7c. Load path through spine bracing	24
Figure 8. Shear forces applied to the top plan bracing (S_a)	24
Figure 9b. Shear forces resisted by flexural stiffness of uprights (S_f)	25
Figure 10. Horizontal force applied to top of spine bracing (S_s)	26
Figure 11. Pallet rail beam force to spine bracing	26
Figure 12. Pallet rail beam forces	27
Figure 13. FBD of 2 bays plan bracing	27
Figure 14. FBD of 5 bays plan bracing	28
Figure 15. FBD of 8 bays plan bracing (2 bracing bays)	28
Figure 16. Forces applied to plan bracing	29
Figure 17. Deformations of top level of frame	29
Figure 18. Deflected shape of top plan bracing	30

1 Introduction

Steel storage racks are widely used in the storage industry for storing palletized goods. Rack structures normally consist of light gauge cold-formed steel members that are used as columns, beams and bracing.

There are two basic types of storage racking, namely selective racks and drive-in/drive-through racks. Each system has certain advantages and its usage is much depending on its intended application and storage space requirements. Selective racks are usually one or two pallets deep with pallets sitting on top of beams spanning in the down-aisle direction, as shown in figure 1a. Forklift access is allowed along the aisles between rows of racks. This type of rack has been subjected to a wide range of research [1, 2] and its design procedures are covered in various standards [3-5], and reference documents [6-8].

The second type of storage racking, drive-in/drive-through racks, are typically deeper than selective racks with rails mounted in the cross-aisle direction to support the pallets, as shown in figure 1b. This kind of configuration allows a more efficient utilization of storage space with the trade off of reduced accessibility compared to the selective racks. In term of structural stability, it is more prone to buckling in the down-aisle direction due to considerably longer unrestrained length of the uprights. Drive-in and drive-through racks are also susceptible to horizontal impact forces because they do not have the pallet beams tying the uprights together. On the contrary to selective racks, design guidelines for drive-in and drive-through racks are not readily available and limited to the SEMA [9] code of design, which has been available in many years, the draft FEM [10] standard and some limited published research papers [11].

A high number of recent failures of drive-in racks in conjunction with the limited knowledge of this kind of structure as mentioned above have triggered further investigation into the structural behaviour and stability of these racks. Amongst those incidents involving drive-in racks, a majority has emerged from forklifts hitting the uprights with subsequent progressive dislodgement of pallets down through the bay and a localised failure of the uprights surrounding the bay. Impact forces may also result in overstressing the bracing systems which then lead to the global collapse of the entire structure.

This paper is concerned with the structural behaviour and design of drive-in racks. Particular attention is paid to the load path through the drive-in rack system of horizontal impact forces applied in the down-aisle direction.

2 Methodology

A typical finite element analysis model of a drive-in rack system was constructed using the Strand7 [12] FEA package and analysed with a nominal 1000 N horizontal force applied at the half-height of the outer-most upright. The load path through the structure is investigated with attention given to the displacements and forces developing in the plan bracing and spine bracing systems. Sensitivity studies are conducted to investigate how varying the number of bays in the down-aisle direction affects the distribution of forces transferred through the bracing systems. Finally, a simplified mechanical model is developed for the prediction of

displacements and internal forces arising from horizontal impact loads. The model is based on the 2D model suggested by Godley [11].

3 Finite element model

3.1 Geometry and Element Types

A typical finite element analysis model of a 5 bay drive-in rack with two pallet levels was constructed using beam-line elements. Figures 2 and 3 show the general arrangement of the drive-in rack system. A special type of beam-line element, named as “cut-off” bar, was used to represent the bracing elements, which were rigidly connected to uprights. During the analysis, these bracing elements only supported tension forces. For elements in compression, they became inactive, or in other words, were removed from the system.

For this study, the top plan portal beams were assumed to be semi-rigidly connected to the top of the uprights via partial rotational end-release at the ends of the beam elements. The value of this rotational stiffness is 35 kNm/rad and was determined experimentally [13]. A similar approach was used for the rotational stiffness at the base of the uprights for flexure in the down-aisle direction with the stiffness value taken as 156 kNm/rad as described in [14]. The pallet runner beams were assumed to be pin-connected to the support cantilevers.

The frame was assumed to be simply supported at the base of the uprights in the cross-aisle direction.

An out-of-plumb of 0.002 was also applied to the model in the down-aisle direction as required by the FEM standard [10].

3.2 Materials

All structural steel components of the drive-in rack model are made from structural steel with Young modulus $E = 200$ GPa, Poisson ratio $\mu = 0.3$, density $\rho = 7850$ kg/m³.

The properties of each type of element are given in Table 1 and its associated figures 4-6.

3.3 Loading

As mentioned previously, the only load applied to the drive-in rack model for this study was a static horizontal impact load of 1000N in the down-aisle direction. This load was applied at the mid-height of the exterior front row upright.

4 Analysis results

4.1 Load path

The FEA model was analysed using Strand7 assuming a geometric nonlinear and a linear-elastic material response. The load path through the rack system from the down-aisle horizontal load is shown in figures 7a to 7c.

The horizontal load was transferred through bending action in the loaded upright to the first and second pallet levels underneath and above the loading point at approximately a half-to-half ratio. At these levels, the bending stiffness of the pallet runner beam helps distributing the force to the internal uprights. The shear forces at the bottom level were then transferred to the base of the uprights and to the ground. For the upper level, the shear forces were transferred to the top plan bracing and the portal beams.

The shear forces transferred at the top level were partly resisted by the stiffness of the uprights against bending in the down-aisle direction. All uprights were connected in the down-aisle direction by the connecting portal beams. The rest of the force was transferred through the truss action of the plan bracing system to the top of the spine bracing. This component of the applied force then traveled down to the base of the uprights in the rear plane by the truss action of the spine bracing.

It has been noted from the force diagram that the pallet runner beams play a significant role in the load transfer through the system. At the rear end adjacent to the spine bracing, the pallet rail beam connected to the loaded upright applies a shear force in the opposite direction to the applied external force as shown in figure 7c, and hence significantly reduces the axial forces transferred through the spine bracing.

4.2 Sensitivity study results

Analyses were carried out for a series of drive-in racks with the number of bays in the down-aisle direction varying from 2 to 8. Additional cases were considered for 8 and 11 bay racks with double plan and spine bracing systems installed at each end of the structure. In all analyses, the applied force was 1000 N.

- Forces applied to top plan bracing, S_a

The shear forces transferred to the top plan bracing for various numbers of bay configurations are shown in figure 8. Observation of the graph indicates that the forces transferred to the top plan bracing are approximately independent of the number of bays in the down-aisle direction. The average magnitudes of the forces applied to the plan bracing are

$$\begin{aligned} P_1 &= 0.23 P \\ P_2 &= 0.18 P \\ P_3 &= 0.08 P \\ P_4 &= 0.025 P \\ P_5 &= -0.002 P \\ P_6 &= -0.006 P \\ P_7 &= -0.007 P \end{aligned}$$

where P_1 is the shear force transferred from the front upright to the plan bracing, P_7 is the shear force transferred at the rear upright and P is the applied horizontal force.

- Forces resisted by the flexural stiffness of uprights in down-aisle direction, S_f

The total shear forces resisted by the flexural stiffness of the uprights in the down-aisle direction are displayed in figures 9a and 9b. These forces are the sums of the shear forces transferred from the portal beams into the uprights not including the impacted upright and the

row this upright is connected to via the beam rails, and not including the uprights connected to the spine bracing. Figure 9a shows the total shear force resisted for each system configuration along the depth of the rack (frame 1 at front and frame 7 at rear). Figure 9b displays the total shear force resisted at each upright position along the depth of the rack with the x-axis being the number of bays in the down-aisle direction. The graph shows that the magnitude of the total shear force increases with the number of bays in the down-aisle direction as one would expect. The shear forces also vary almost linearly from the front to the rear of the rack frame, as shown in figure 8. For the cases with double bay bracing configuration, the slope from front to rear is steeper.

- Force applied to top of spine bracing, S_s

The total horizontal force applied to the top of the spine bracing for different numbers of bay configurations are shown in figure 10. This force is the shear force transferred at the top of the third upright forming part of the spine bracing. The trend line indicates that the higher the number of bays in the down-aisle direction, the lesser the force is transferred to the spine bracing. In other words, the flexural stiffness of the uprights in the down-aisle direction has a more significant role for drive-in racks with a large number of bays.

- Pallet beam forces

Figure 11 shows the magnitude of the horizontal shear force in the pallet rail beams at the rear end joining the spine bracing system, as shown in figure 12. It can be observed that the magnitudes of the shear forces at both upper and lower pallet level are essentially independent of the number of bays in the down-aisle direction. Furthermore, the magnitude of the beam rail shear forces transferred to the internal upright at the rear (upright 3) is much smaller than that transferred to the exterior upright at the rear (upright 1).

- Free Body Diagram (FBD) visualization

Free Body Diagrams (FBD) of the top level of the frame for 2 bay, 5 bay and 8 bay (doubly braced) systems are shown in figures 13, 14 and 15 respectively. The shear forces in the uprights just below the top plan bracing are visualized in the FBDs. The forces include those applied to the exterior row of uprights (S_a), the resultant (S_f) of the shear forces in the uprights arising from flexure in the down-aisle direction, and the shear force (S_s) in the third upright at the rear which forms part of the spine bracing. The shear forces S_a are in equilibrium with the sum of the shear forces S_f and S_s .

5 Mechanical model

5.1 Development of model

A simple mechanical model of the drive-in rack has been constructed based on the “single column model” suggested by Godley [11]. In the model, the loads are applied to the top plan bracing according to a triangular distribution such that the sum of these forces equals to half of the applied horizontal impact force and are denoted by P_1 to P_7 as shown in figure 16. These applied forces can be evaluated from equation (1),

$$P_i = \frac{(N_u - i)P}{(N_u - 1)N_u} \quad (1)$$

where N_u is the number of uprights in the cross-aisle direction, and

$$\sum_i P_i = \frac{P}{2} \quad (2)$$

The deflection of the front face of the rack under the action of the loads shown in figure 16 is denoted by Δ_l . This deflection is composed of contributions from deformations of the spine bracing and uprights (Δ_s), cross and down-aisle deformations of the uprights resulting from the rotation of the plan bracing (Δ_r) and deformations of the plan bracing (Δ_p). These contributions are shown in figures 17a – 17c.

Part of the total force $F_a = \sum P_i = P/2$ is transferred to the top of the spine bracing, the rest is resisted by the stiffness of the uprights in the down-aisle direction. Denoting the force applied to the spine bracing system by $F_s = (1 - \beta) P / 2$, the horizontal displacement of the rack due to spine bracing deformation is determined from

$$\Delta_s = \frac{F_s H}{E} \left\{ \frac{1}{A_s \sin \alpha_s \cos^2 \alpha_s} + \frac{\tan^2 \alpha_s (2(N_s + 1)^2 + 1)}{3A_c} \right\} \quad (3)$$

where Δ_s is defined in figure 17a. The derivation of equation (3) is shown in Appendix B. In equation 3, $A_s E$ is the axial rigidity of the spine bracing diagonals and α_s their angle of inclination with horizontal. The second term in the equation caters for the effect of axial deformations of the vertical uprights which form part of the spine bracing system.

In determining the contribution Δ_p from deformations of the top plan bracing system, as shown in figure 17c, the bracing is assumed to behave linearly and members are taken to be pin-jointed and supporting tension only. The contribution is,

$$\Delta_p = \frac{\sum_{i=1}^7 (1 - \beta) P_i h_i}{A_p E \sin \alpha_p \cos^2 \alpha_p + A_h E \tan \alpha_p} \quad (4)$$

in which $A_p E$ is the axial rigidity of the plan bracing diagonals, $A_h E$ is the axial rigidity of the plan bracing horizontal beam and α_p is the angle of inclination of the diagonals. The coefficient β denotes the portion of force resisted by the flexural stiffness of the uprights in the down-aisle direction.

The plan bracing is supported by the top of the uprights and, under horizontal down-aisle loads, tends to rotate as shown in figure 18. The resistance to this rotational movement is provided mainly by the two rows of uprights to which the plan bracing is connected, as shown in figure 17b.

Due to the action of the horizontal force F_s , the resultant forces F_v on the two end rows are

$$F_v = \frac{F_s L_d}{L_b} \quad (5)$$

where L_d and L_b are the width and length of the top plan bracing, as shown in figure 17c, and the line of action of F_s is taken at the front of the rack.

The force F_v produces a deflection at the top of the upright frame of

$$\Delta_f = \frac{2F_v H}{(N_u - 1)E} \left(\frac{1}{A_f \sin \alpha_f \cos^2 \alpha_f} + \frac{\tan^2 \alpha_f (2(N_{fv} + 1)^2 + 1)}{3A_c} \right) \quad (6)$$

in which N_u is the number of uprights in the cross-aisle direction, N_{fv} is the factor such that $N_{fv} = H/h - 1$ where h is the half the distance between two brace points in the cross-aisle direction, $A_f E$ is the axial rigidity of the cross bracing diagonals and α_f their angle of inclination with horizontal.

The resulting rotation of the plan bracing ϕ is

$$\phi = \frac{2\Delta_f}{L_b} \quad (7)$$

Hence, assuming the frame rotates about a point located at the rear of the rack, the deflection in the down-aisle direction at the front face of the rack is

$$\Delta_\phi = \phi L_d = \frac{2F_s H L_d^2}{(N_u - 1)L_b^2 E} \left(\frac{1}{A_f \sin \alpha_f \cos^2 \alpha_f} + \frac{\tan^2 \alpha_f (2(N_{fv} + 1)^2 + 1)}{3A_c} \right) \quad (8)$$

The total horizontal deflection at the top of the upright from front to rear of the rack is given by

$$\Delta_i = \Delta_s + (\Delta_p + \Delta_\phi) \frac{N_u - i}{N_u - 1} \quad (9)$$

The total force resisted by the uprights in the down-aisle direction can be calculated as

$$F_f = (N_v - 1) \sum \frac{3EI_c \Delta_i}{H^3} \mu_s = \beta F_a = \beta \frac{P}{2} \quad (10)$$

where μ_s is the factor accounting for the semi-rigidity of the joints at the base (K_b) and between uprights and portal beams (K_t) and is evaluated from the following equation

$$\mu_s = \frac{12EI_c (K_t + K_b) + \frac{K_t K_b I_c}{I_b} \left(\frac{L_b}{2} \right) + 12K_t K_b H}{12EI_c (K_t + K_b) + \frac{K_t K_b I_c}{I_b} \left(\frac{L_b}{2} \right) + 3K_t K_b H + 36 \frac{(EI_c)^2}{H} + 3 \frac{EI_c}{H} \frac{K_t L_b I_c}{2I_b}} \quad (11)$$

as derived in Appendix C. Hence,

$$\beta = \frac{2(N_v - 1) \sum_{i=1}^{N_b} \frac{3EI_c \Delta_i}{H^3} \mu_s}{P} \quad (12)$$

where N_v is the number of uprights in the down-aisle direction

The process can be iterated until convergence is satisfied for the value of β .

5.2 Worked example

The above procedure is applied to the 5 bays long drive-in rack also analyzed in the FEA model. As per equation (1), the forces applied to the top plan bracing due to 1000N horizontal impact load are

$$\begin{aligned} P_1 &= 142.9 \text{ N} \\ P_2 &= 119.0 \text{ N} \\ P_3 &= 95.2 \text{ N} \\ P_4 &= 71.4 \text{ N} \\ P_5 &= 47.6 \text{ N} \\ P_6 &= 23.8 \text{ N} \\ P_7 &= 0.0 \text{ N} \end{aligned}$$

Try $\beta = 0.6$

$$\begin{aligned} A_p &= 156 \text{ mm}^2 \\ \alpha_p &= 0.676 \text{ radian} \\ A_h &= 275 \text{ mm}^2 \\ (\text{Equation 2}) \Delta_p &= 0.0181 \text{ mm} \\ A_s &= 250 \text{ mm}^2 \\ \alpha_s &= 0.811 \text{ radian} \\ N_s &= 2 \\ H &= 9.075 \text{ m} \\ A_c &= 780 \text{ mm}^2 \\ (\text{Equation 3}) \Delta_s &= 0.187 \text{ mm} \end{aligned}$$

$$\begin{aligned} (\text{Equation 4}) F_v &= 480.8 \text{ N} \\ A_f &= 10 \text{ mm}^2 \\ \alpha_f &= 0.474 \text{ radian} \\ N_u &= 7 \\ N_{fv} &= 13 \\ (\text{Equation 5}) \Delta_f &= 2.29 \text{ mm} \\ (\text{Equation 6}) \phi &= 0.00157 \text{ radian} \\ (\text{Equation 7}) \Delta_\phi &= 11.03 \text{ mm} \end{aligned}$$

Hence, the deflection at front face of the rack is

$$\begin{aligned} (\text{Equation 8}) \Delta_i &= 11.24 \text{ mm} \\ I_c &= 1.165 \times 10^6 \text{ mm}^4 \end{aligned}$$

$$I_b = 0.311 \times 10^6 \text{ mm}^4$$

$$N_v = 6$$

$$\text{(Equation 9) } F_f = 283.8 \text{ N}$$

$$\text{where } \alpha_s = 1.525 \text{ from (Equation 10)}$$

$$\text{(Equation 11) } \beta = 0.568$$

It can be observed that for the first iteration, the calculated coefficient β is slightly less than the trial value β .

Try $\beta = 0.586$ for second iteration. Once again, we have

$$\text{(Equation 2) } \Delta_p = 0.0187 \text{ mm}$$

$$\text{(Equation 3) } \Delta_s = 0.194 \text{ mm}$$

$$\text{(Equation 4) } F_v = 497.7 \text{ N}$$

$$\text{(Equation 5) } \Delta_f = 2.37 \text{ mm}$$

$$\text{(Equation 6) } \phi = 0.00163 \text{ radian}$$

$$\text{(Equation 7) } \Delta_\phi = 11.41 \text{ mm}$$

Hence, the deflection at front face of the rack is

$$\text{(Equation 8) } \Delta_i = 11.63 \text{ mm}$$

$$\text{(Equation 9) } F_f = 293.7 \text{ N}$$

$$\text{(Equation 11) } \beta = 0.587$$

For this iteration, the calculated coefficient β is similar to the trial value, hence the result is considered to be converged.

The deflection at front face of the rack from the FEA model is 13.9mm which differs by less than 16% from the value (11.63mm) obtained from the mechanical model. The shear forces F_s and F_f from the FEA model are 146 N and 354 N respectively as compared to the values of 207 N and 297 N obtained from the theoretical model. It can be noted from the above results that the front face deflection of the rack is governed by the rotation of the plan bracing which in turn is controlled by the deflection of the cross-aisle frame.

6 Conclusions

This report explains the load transfer mechanism of horizontal forces in typical drive-in racking structures by the use of FEA modelling. A series of sensitivity studies with different rack configurations has shown that the stiffness of the uprights in the down-aisle direction has a significant role in transferring the horizontal load. It is also found that the forces developing in the spine bracing system are influenced considerably by the action of the pallet runner beams. An enhanced mechanical design model based on the “single column model” suggested by Godley [11] is proposed for determining deformations and internal forces in drive-in racking systems subjected to horizontal impact forces. The results obtained from the design model are reasonably close to the results of the FEA model.

7 References

1. Sarawit, A. and T. Pekoz. *Design of Industrial Storage Racks*. in *16th International Conference on Cold-formed Steel Structures*. 2002. Orlando.
2. Davies, J.M. *Down-isle Stability of Rack Structures*. in *11th International Conference of Cold-formed Steel Structures*. 1992. St Louis.
3. AS4084, *Steel Storage Racking*. 1993, Standards Australia: Sydney.
4. RMI, *Specification for the Design, Testing and Utilization of Steel Storage Racks*. 1997, Rack Manufacturers Institute: Charlotte NC.
5. FEM, *Recommendations for the Design of Steel Static Pallet Racking and Shelving, Section X*. 1998, Federation Europeenne de la Manutention: Brussels.
6. Davies, J.M., *Pallet Racking*, in *Light Gauge Metal Structures, Recent Advances*, J.R.a.D. Dubina, Editor. 2005, Springer: Vienna. p. 233-253.
7. Hancock, G.J., T.M. Murray, and D.S. Ellifrit, *Cold-formed Steel Structures to the AISI Specification*. 2001, New York: Marcel Dekker, Inc.
8. Godley, M.H.R., *Storage Racking*, in *Design of Cold-formed Steel Members*, J. Rhodes, Editor. 1991, Elsevier Applied Science: London.
9. SEMA, *Code of Practice for the Design of Static Racking*. 1980, Storage Equipment Manufacturers Association.
10. FEM, *The design of drive-in and drive through storage racking, FEM 10.2.07*. Version 0.02 ed. Drive in design code. 2002: Federation Europeene de la Manutention.
11. Godley, M.H.R. *The Behaviour of Drive-in Storage Structures*. in *16th International Specialty Conference on Cold-formed Steel Structures*. 2002. Orlando.
12. Strand7, *Theoretical Manual*. 2005, Sydney: G&D Computing.
13. Moll, Ing. R., *Box Beam to Upright Connection*. 2002, Institut für Schweißtechnik und Ingenieurbüro Dr. Möll GmbH.
14. Moll, Ing. R., *Floor Connection Tests*. 2002, Institut für Schweißtechnik und Ingenieurbüro Dr. Möll GmbH.
15. CASE, *Determination of the Shear Stiffness of Upright Frames, S1207*. 1999, Centre for Advanced Structural Engineering, University of Sydney: Sydney.

Appendix A: Notation

A_c	Cross-sectional area of upright
A_f	Cross-sectional area of cross-aisle frame bracing diagonal
A_p	Cross-sectional area of plan bracing diagonal
A_s	Cross-sectional area of spine bracing diagonal
β	percentage of shear force resisted by flexural stiffness of uprights
α_f	angle of inclination of cross-aisle frame bracing diagonal
α_p	angle of inclination of plan bracing diagonal
α_s	angle of inclination of spine bracing diagonal
Δ_i	horizontal displacement of the upright at row i
Δ_ϕ	horizontal displacement due to rigid body rotation of the plan bracing
Δ_f	horizontal displacement of the cross-aisle frame bracing
Δ_p	horizontal displacement of the plan bracing
Δ_s	horizontal displacement of the spine bracing
E	Elastic modulus
ϕ	rigid body rotation of the plan bracing
F	total load applied to plan bracing
F'	load transferred to spine bracing
F''	load resisted by upright stiffness in down-aisle direction
F_v	horizontal load on cross-aisle frame bracing
H	rack height
I_b	second moment of area of the portal beam
I_c	second moment of area of the upright
K_b	joint rotational stiffness between upright and the base
K_t	joint rotational stiffness between upright and portal beam
L_b	width of plan bracing
L_d	depth of plan bracing
μ	Poisson ratio
N_u	number of upright in the cross-aisle direction
N_v	number of upright in the down-aisle direction
ρ	density

Appendix B: Derivation of spine bracing distortion

N_s = number of pallet level

A_c = cross sectional area of upright

A_s = cross section area of cross brace

$$h = \frac{H}{(N_s + 1)}$$

$$L_b = \frac{h}{\tan \alpha_s} = \frac{H}{(N_s + 1) \tan \alpha_s}$$

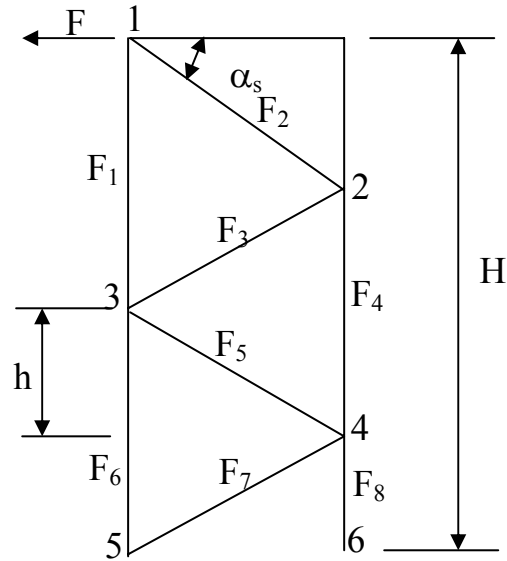
$$F_1 = F \tan \alpha_s$$

$$F_2 = F_3 = F_5 = F_7 = \frac{F}{\cos \alpha_s}$$

$$F_4 = (F_2 + F_3) \sin \alpha_s = 2F \tan \alpha_s$$

$$F_6 = F_1 + (F_3 + F_5) \sin \alpha_s = 3F \tan \alpha_s$$

$$F_8 = (N_s + 1)F \tan \alpha_s$$



Applying the method of virtual forces, the displacement Δ_s due to force F can be calculated from

$$\Delta_s = \sum_i N_i \frac{f_i L_i}{EA_i}$$

where f_i = force in member when $F=1$

For member 1-3

$$F_1 \frac{f_1 l_1}{EA_c} = F \tan \alpha_s \frac{\tan \alpha_s \frac{2H}{(N_s + 1)}}{EA_c} = \frac{2FH \tan^2 \alpha_s}{EA_c (N_s + 1)}$$

For member 2-4

$$F_4 \frac{f_4 l_4}{EA_c} = 2F \tan \alpha_s \frac{2 \tan \alpha_s \frac{2H}{(N_s + 1)}}{EA_c} = \frac{2FH (2 \tan \alpha_s)^2}{EA_c (N_s + 1)}$$

For member 3-5

$$F_6 \frac{f_6 l_6}{EA_c} = 3F \tan \alpha_s \frac{3 \tan \alpha_s \frac{2H}{(N_s + 1)}}{EA_c} = \frac{2FH (3 \tan \alpha_s)^2}{EA_c (N_s + 1)}$$

For member 4-6

$$F_8 \frac{f_8 l_8}{EA_c} = (N_s + 1)F \tan \alpha_s \frac{(N_s + 1) \tan \alpha_s \frac{H}{(N_s + 1)}}{EA_c} = \frac{FH ((N_s + 1) \tan \alpha_s)^2}{EA_c (N_s + 1)}$$

For members 1-2, 2-3, 3-4, 4-5

$$F_2 \frac{f_2 l_2}{EA_s} = F_3 \frac{f_3 l_3}{EA_s} = F_5 \frac{f_5 l_5}{EA_s} = F_7 \frac{f_7 l_7}{EA_s} = \frac{F}{\cos \alpha_s} \frac{1}{\cos \alpha_s} \frac{H}{(N_s + 1) \sin \alpha_s} = \frac{FH}{(N_s + 1) EA_s \sin \alpha_s \cos^2 \alpha_s}$$

Hence,

$$\Delta_s = \sum_i N_i \frac{f_i l_i}{EA_i} = (N_s + 1) \frac{FH}{(N_s + 1) EA_s \sin \alpha_s \cos^2 \alpha_s} + \frac{FH}{EA_c} \tan^2 \alpha_s \frac{2}{(N_s + 1)} \left[1^2 + 2^2 + \dots + N_s^2 + \frac{(N_s + 1)^2}{2} \right]$$

$$\text{For } \sum_i^{N_s} i^2 = \frac{N_s (N_s + 1) (2N_s + 1)}{6}$$

The second term in the above equation becomes

$$\begin{aligned} & \frac{FH}{EA_c} \tan^2 \alpha_s \frac{2}{(N_s + 1)} \left[1^2 + 2^2 + \dots + N_s^2 + \frac{(N_s + 1)^2}{2} \right] = \\ & = \frac{FH}{EA_c} \tan^2 \alpha_s \frac{2}{(N_s + 1)} \left[\frac{N_s (N_s + 1) (2N_s + 1)}{6} + \frac{(N_s + 1)^2}{2} \right] \\ & = \frac{FH}{EA_c} \tan^2 \alpha_s \left[\frac{2N_s^2 + 4N_s + 3}{3} \right] = \frac{FH}{EA_c} \tan^2 \alpha_s \left[\frac{2(N_s + 1)^2 + 1}{3} \right] \end{aligned}$$

So,

$$\Delta_s = \frac{FH}{E} \left[\frac{1}{A_s \sin \alpha_s \cos^2 \alpha_s} + \frac{\tan^2 \alpha_s (2(N_s + 1)^2 + 1)}{3A_c} \right]$$

Appendix C: Derivation of stiffness of uprights in the down-aisle direction allowing for semi-rigid joints at the base and at the upright-portal beam connection

θ_b = rotation of beam end center

θ_{ct} = rotation of column at top

θ_{cb} = rotation of column at base

K_t = joint rigidity at top

K_b = joint rigidity at base

$L_b/2$ = distance between uprights in down-aisle direction

$$M_t = 12 \frac{EI_b}{\left(\frac{L_b}{2}\right)^2} \theta_b$$

$$M_t = K_t (\theta_{ct} - \theta_b)$$

Combine (a) and (b)

$$M_t = \frac{K_t \theta_{ct}}{1 + \frac{K_t \left(\frac{L_b}{2}\right)^2}{12EI_b}}$$

$$M_b = K_b \theta_{cb}$$

Slope deflection equation

$$w(x) = L \left(\theta_{cb} + \theta_{ct} - \frac{2\Delta}{H} \right) \left(\frac{x}{H} \right)^3 + H \left(-2\theta_{cb} - \theta_{ct} + \frac{3\Delta}{H} \right) \left(\frac{x}{H} \right)^2 + H\theta_{cb} \left(\frac{x}{H} \right)$$

$$M(x) = -EI_c w''(x)$$

$$M(0) = \frac{2EI_c}{H} \left(2\theta_{cb} + \theta_{ct} - \frac{3\Delta}{H} \right) \quad (e)$$

$$M(H) = -\frac{2EI_c}{H} \left(\theta_{cb} + 2\theta_{ct} - \frac{3\Delta}{H} \right) \quad (f)$$

$$S(x) = -6 \frac{EI_c}{H^2} \left(\theta_{cb} + \theta_{ct} - \frac{2\Delta}{H} \right) x \quad (g)$$

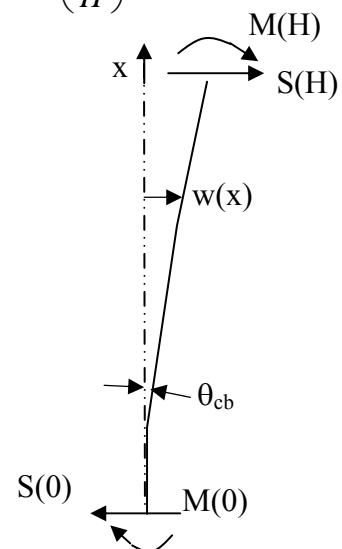
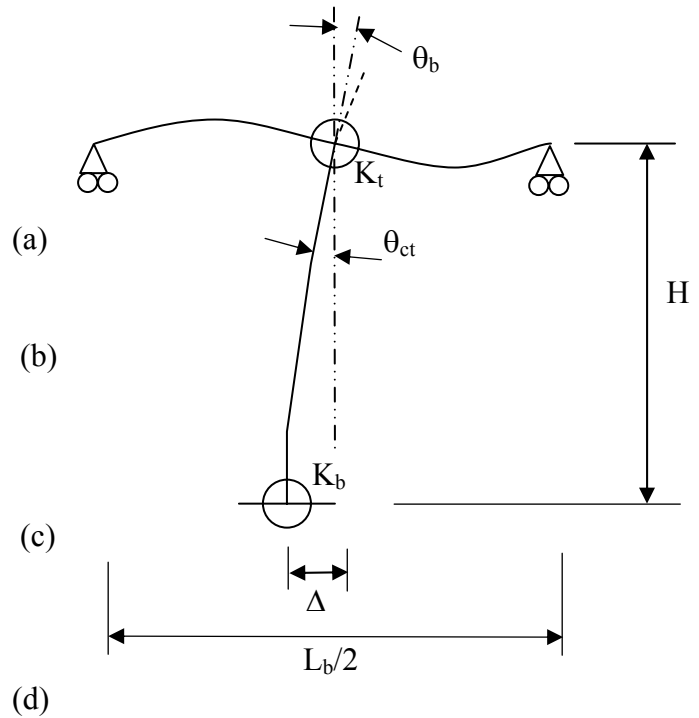
Where

$$M(0) = -M_b \quad (h)$$

$$M(H) = M_t \quad (k)$$

Combine equations (c, d, e, f, g, h, k) and solve for S as a function of Δ

$$S = 3 \frac{EI_c}{H^3} \Delta \mu_s$$



where

$$\mu_s = \frac{12EI_c(K_t + K_b) + \frac{K_t K_b I_c}{I_b} \left(\frac{L_b}{2}\right) + 12K_t K_b H}{12EI_c(K_t + K_b) + \frac{K_t K_b I_c}{I_b} \left(\frac{L_b}{2}\right) + 3K_t K_b H + 36\frac{(EI_c)^2}{H} + 3\frac{EI_c}{H} \frac{K_t I_c}{I_b} \left(\frac{L_b}{2}\right)}$$

Tables

Element Name	Description	Modelling Type
Upright	Standard Siemens Upright RF11024 (figure 4)	Beam
Portal Beam	Standard Siemens Sigma Beam 9016 (figure 5)	Beam
Plan Bracing	26.9 CHS 2.0	Cut off bar – tension only
Spine Bracing	50x5 Flat Bar	Cut off bar – tension only
Cross-aisle Single Frame Bracing	Standard Siemens bracing	Beam Cross Sectional Area = 10.2 mm ²
Cross-aisle Double Frame Bracing	Standard Siemens bracing	Beam Cross Sectional Area = 5.7 mm ²
Pallet Runner	Standard Siemens Pallet Runner (figure 6)	Beam
Pallet Runner Support Cantilever	50x25 Channel	Beam

Table 1: Properties of beam elements

Figures

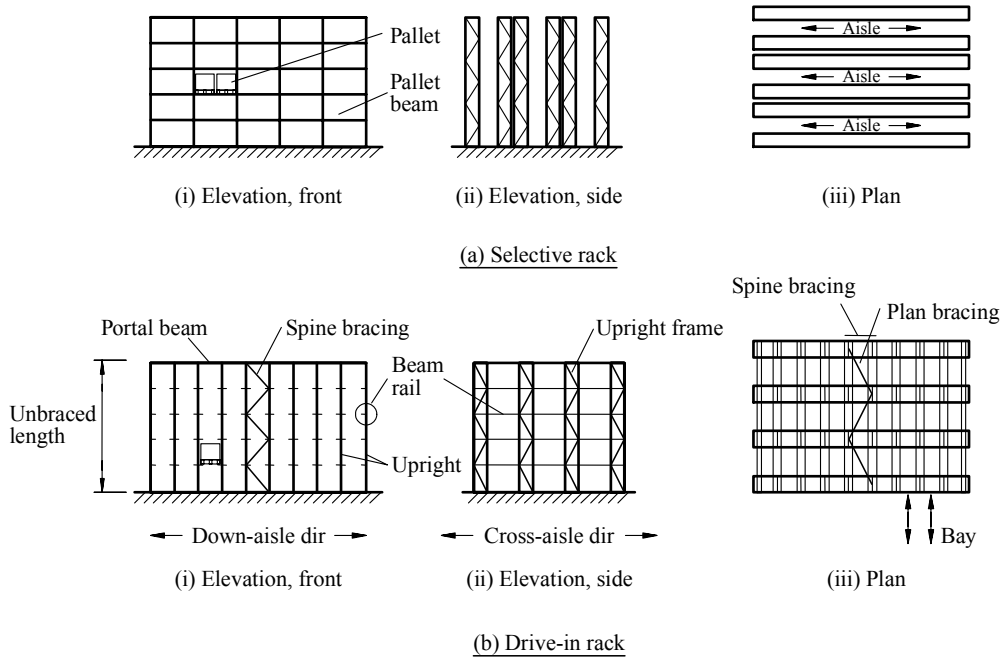


Figure 1. Selective and drive-in rack systems

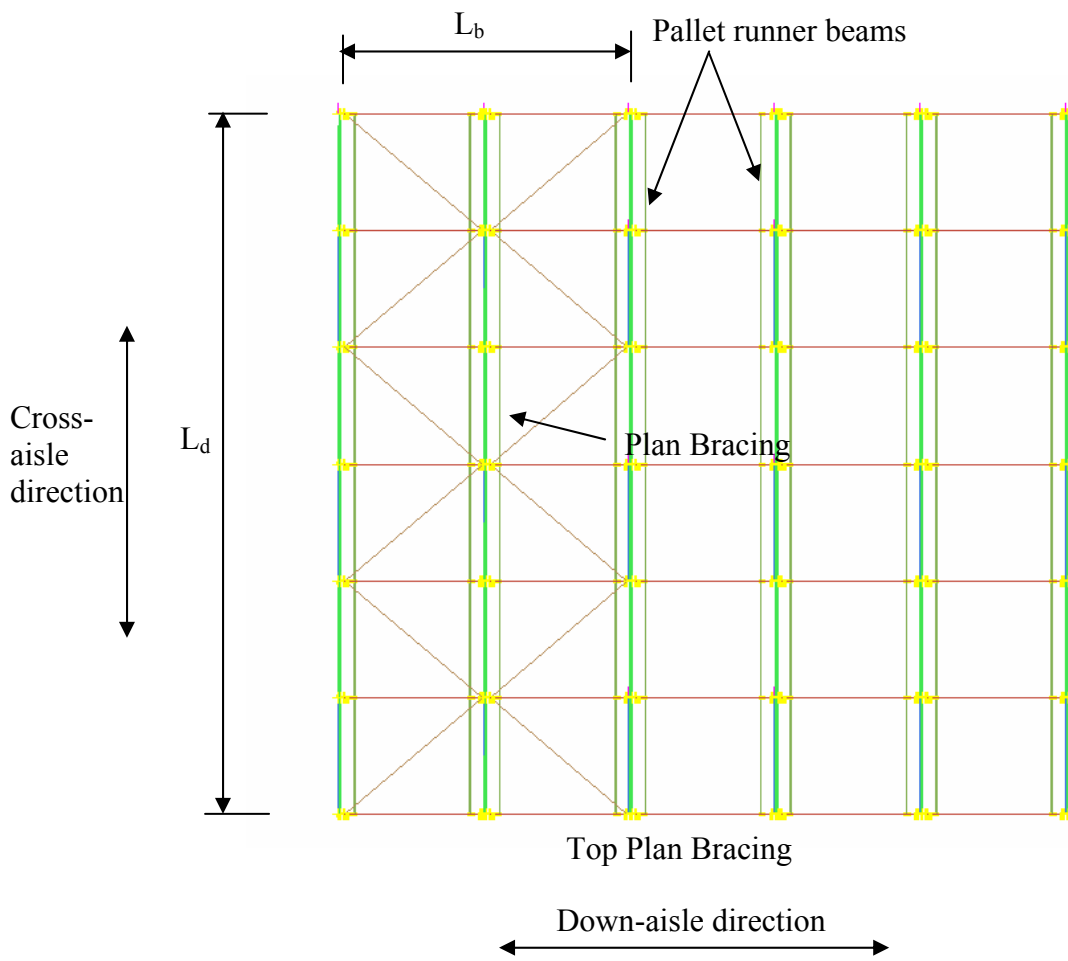
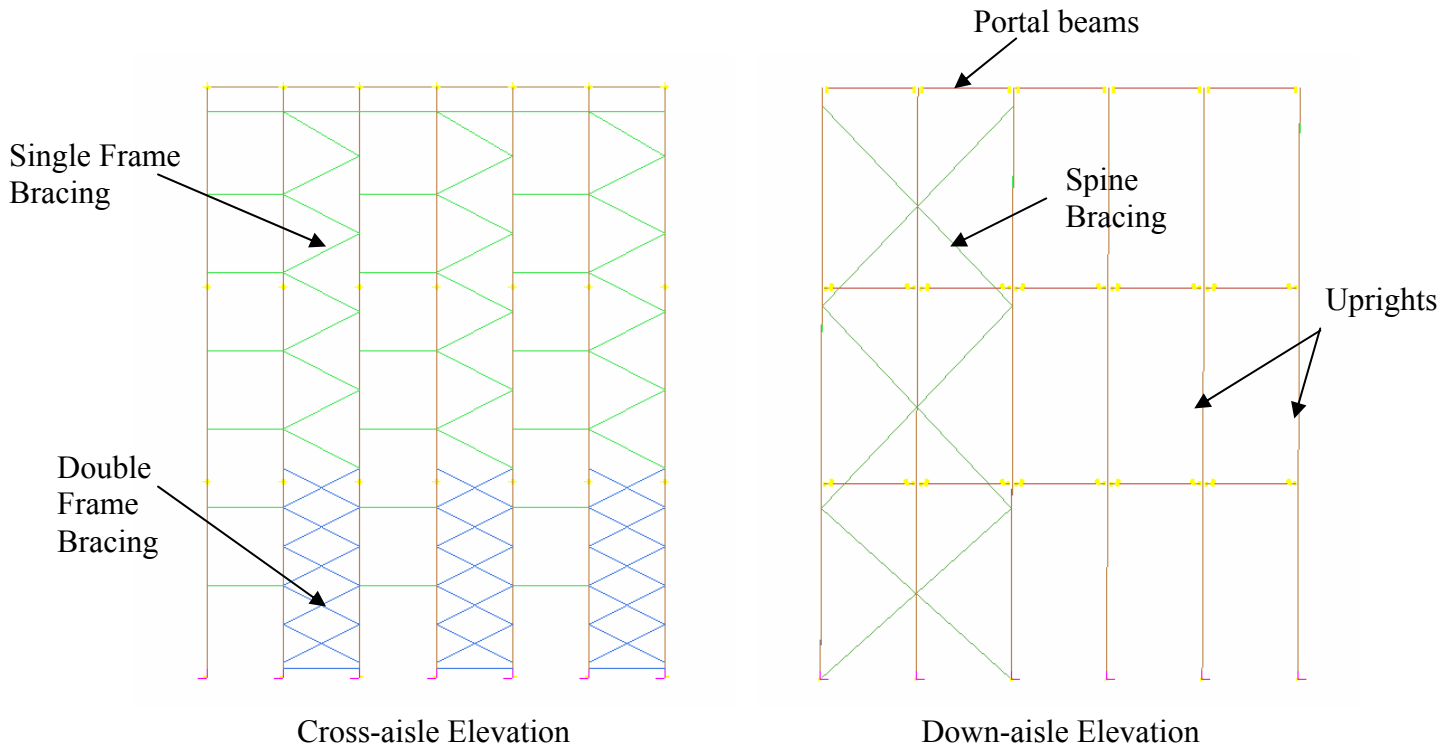


Figure 2. Drive-in Rack Arrangement

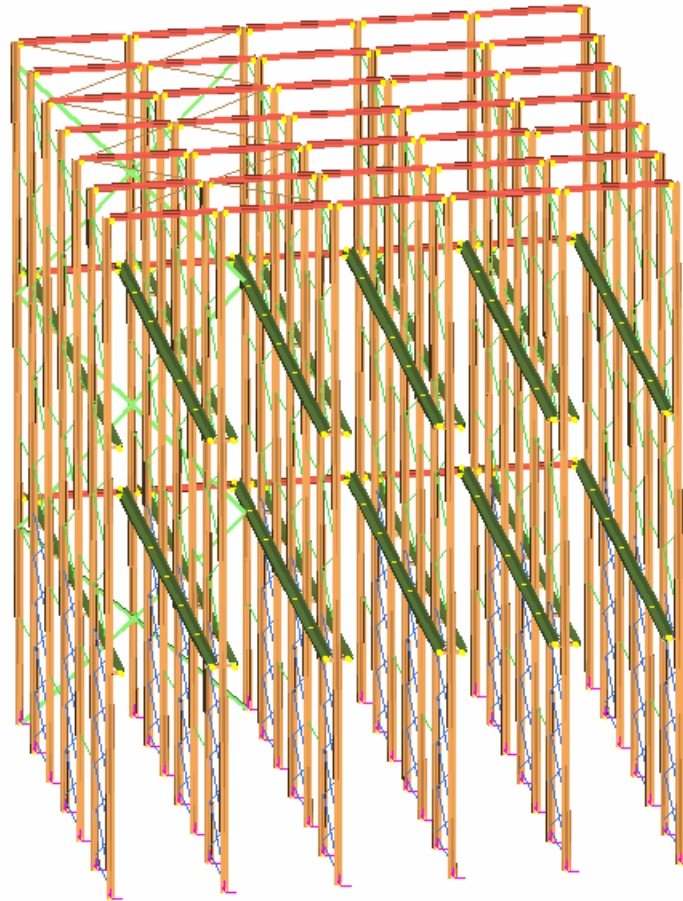


Figure 3. 3D View of Drive-in Rack Model

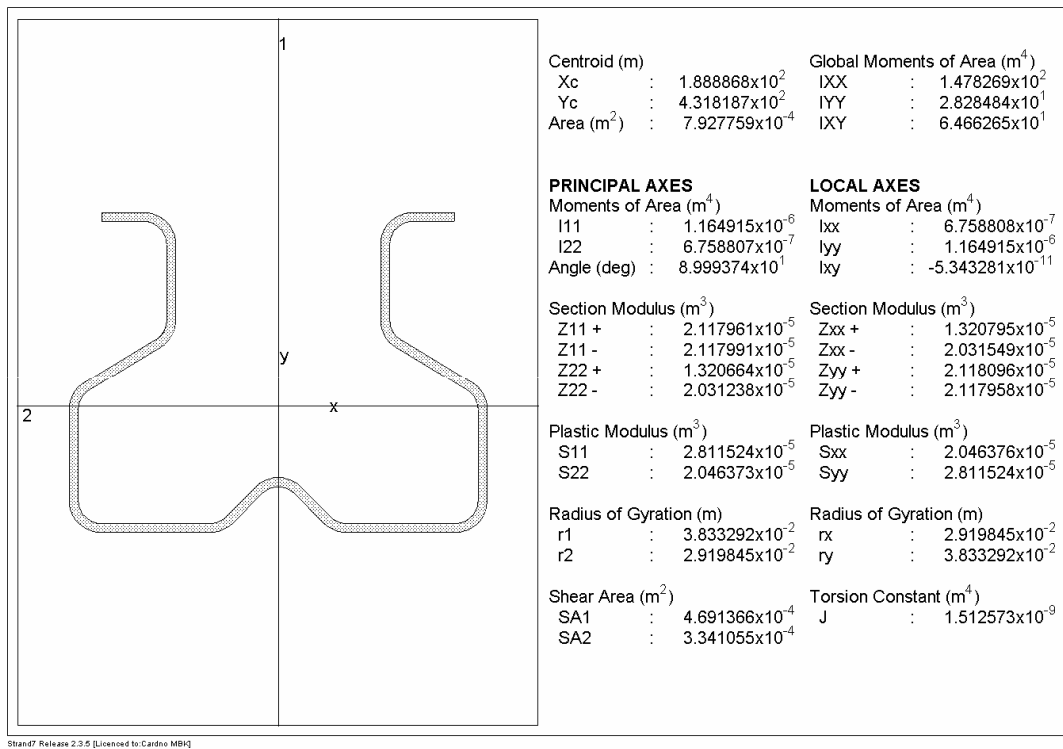
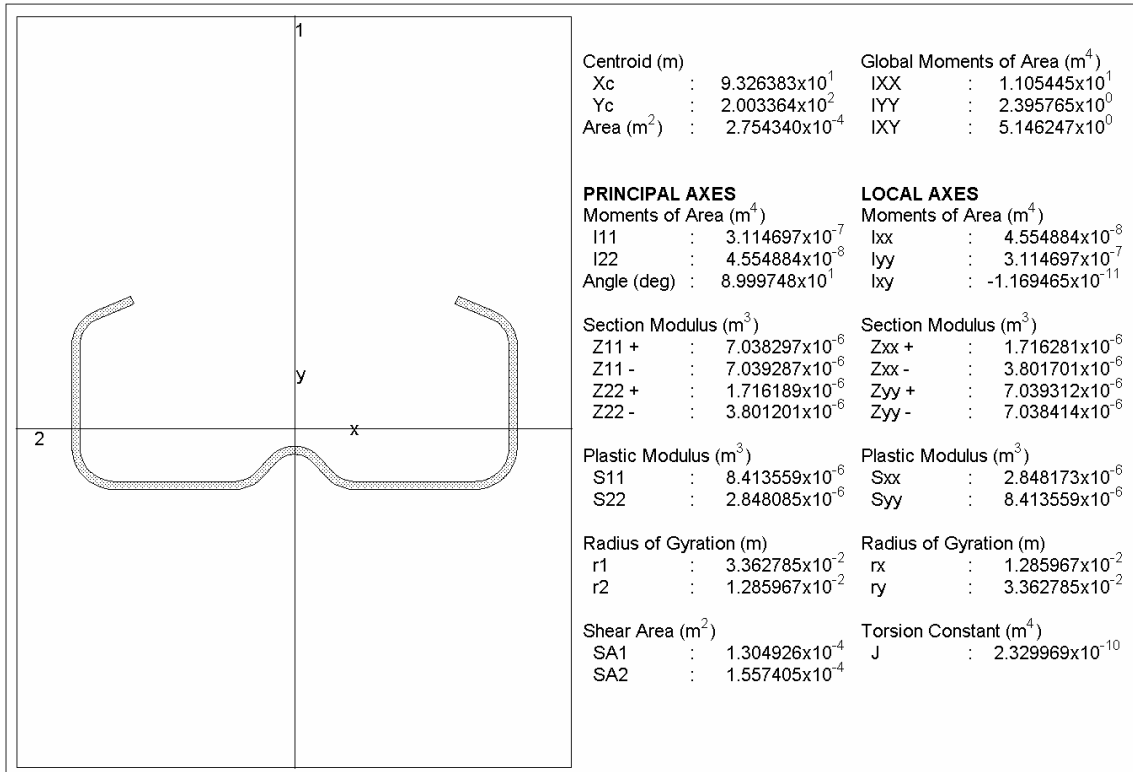
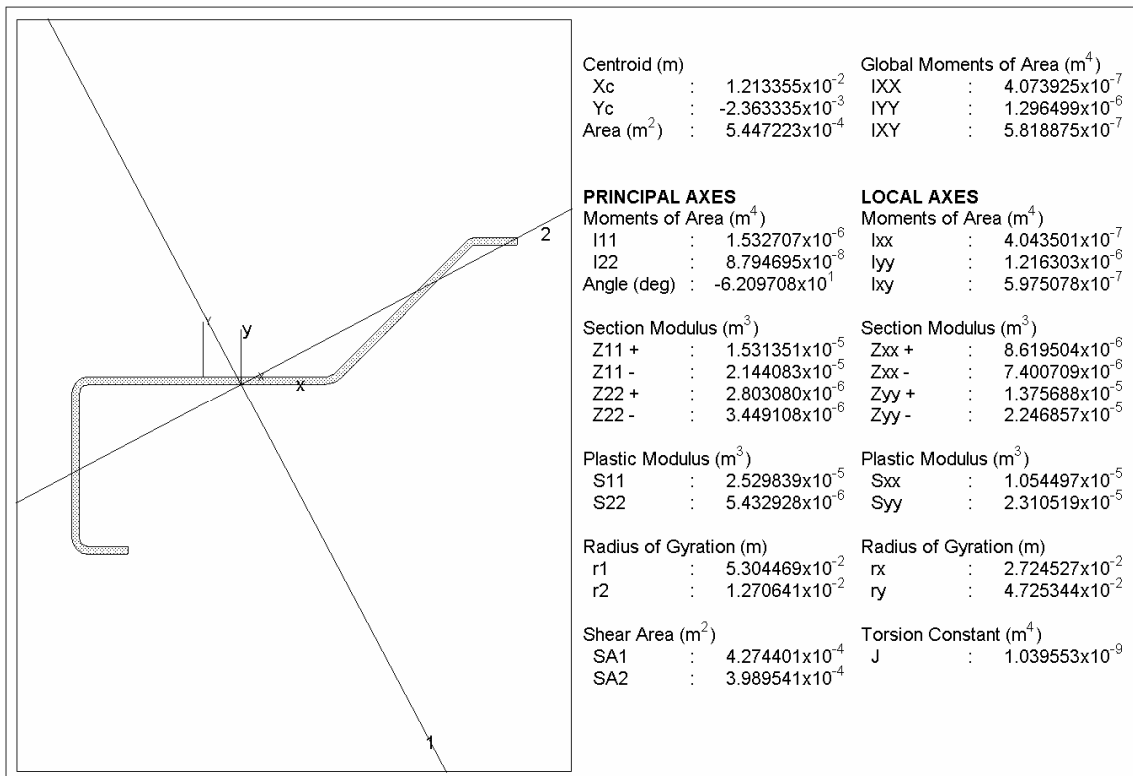


Figure 4. Standard Siemens Upright RF11024



Stand7 Release 2.3.6 [Licenced to:Cardno MBQ]

Figure 5. Standard Siemens Sigma Beam SB9016



Stand7 Release 2.3.6 [Licenced to:Cardno MBQ]

Figure 6. Standard Siemens Pallet Runner

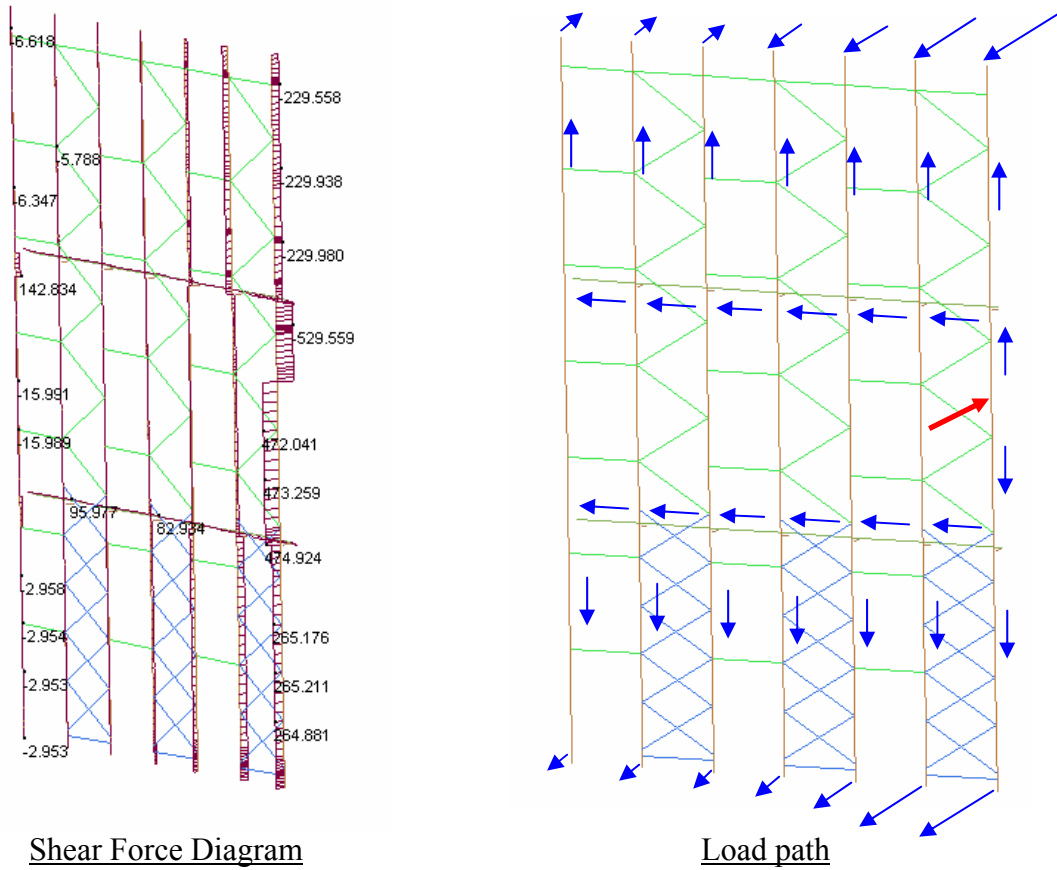


Figure 7a. Load path through front row of drive-in rack

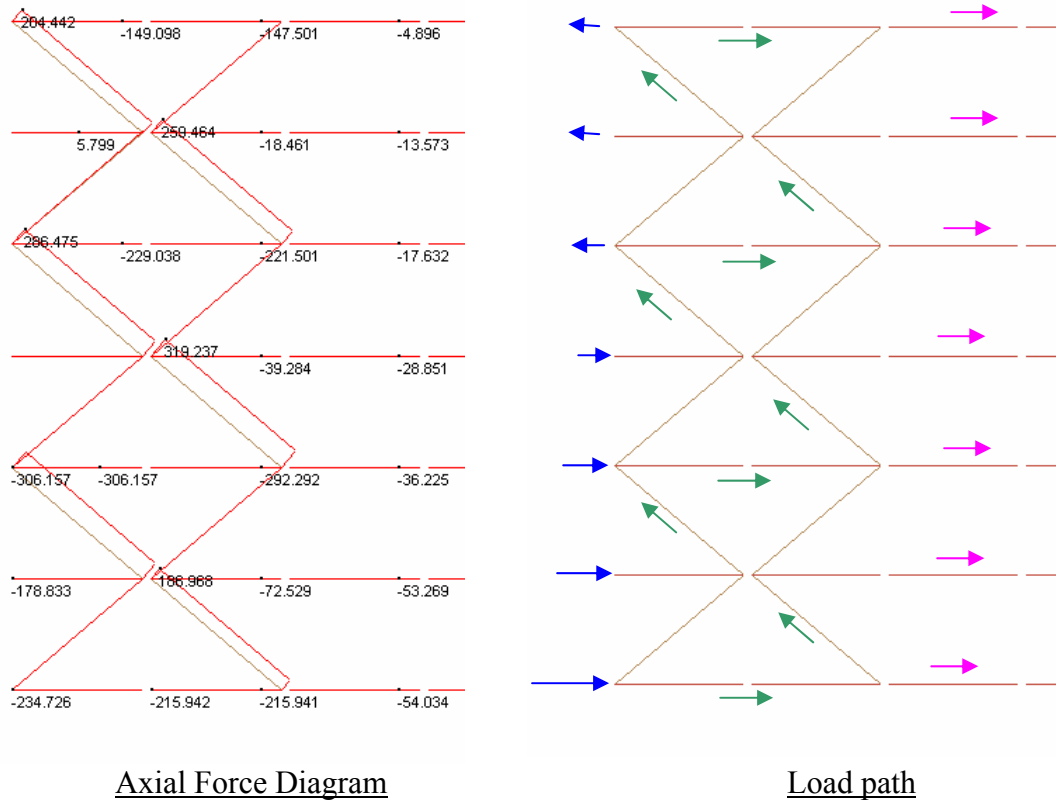


Figure 7b. Load path through top plan bracing

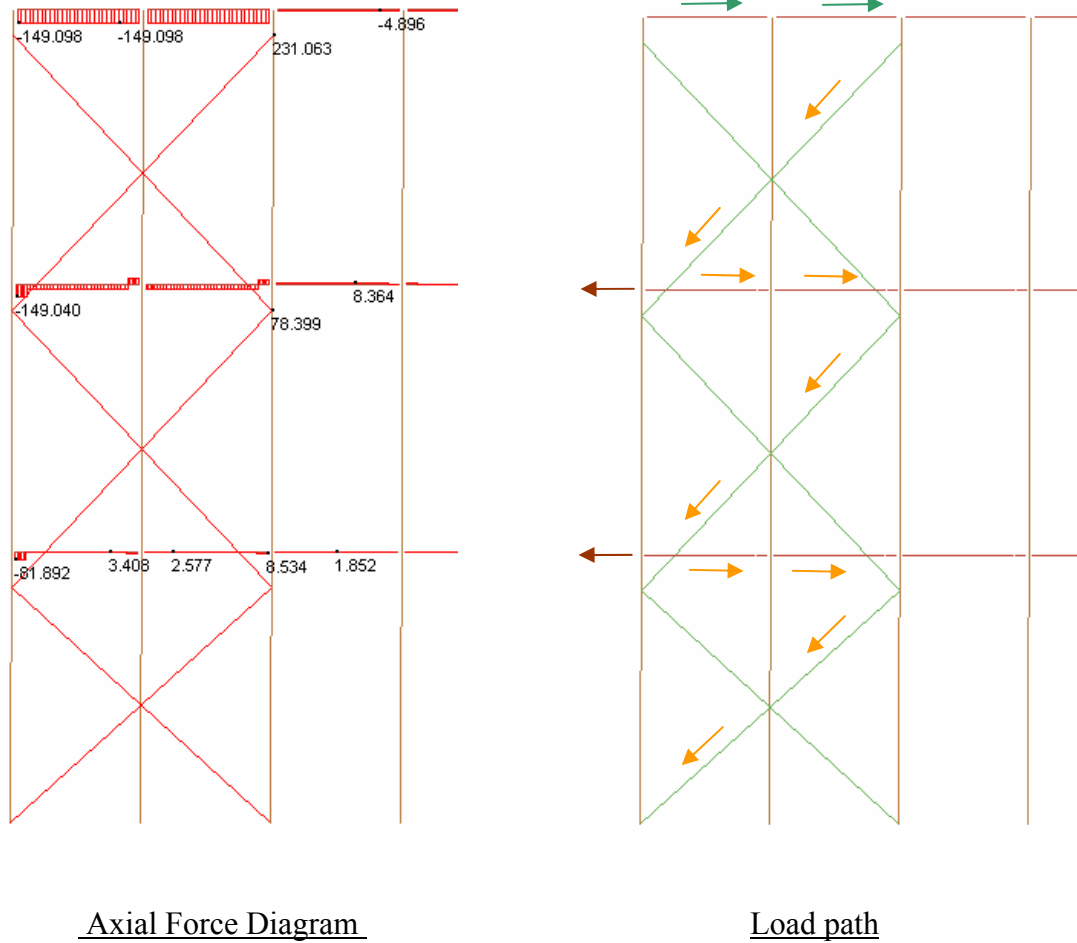


Figure 7c. Load path through spine bracing

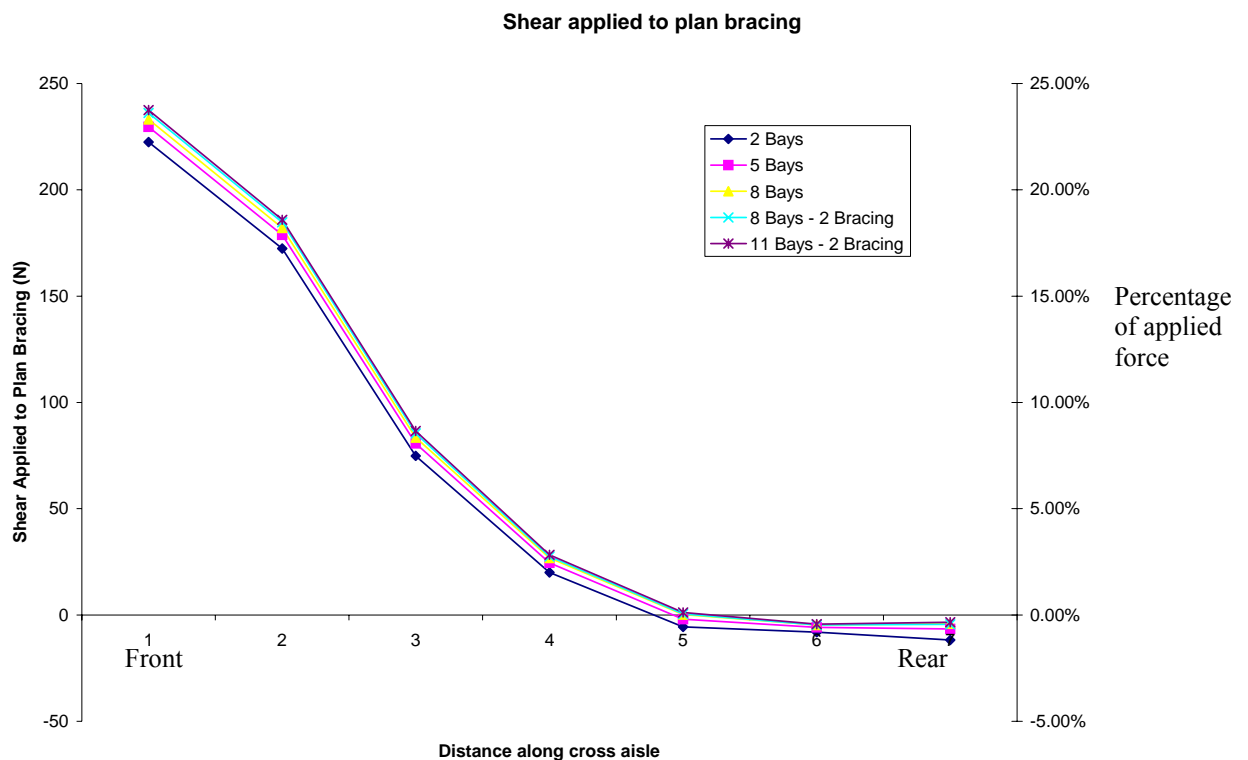


Figure 8. Shear forces applied to the top plan bracing (S_a)

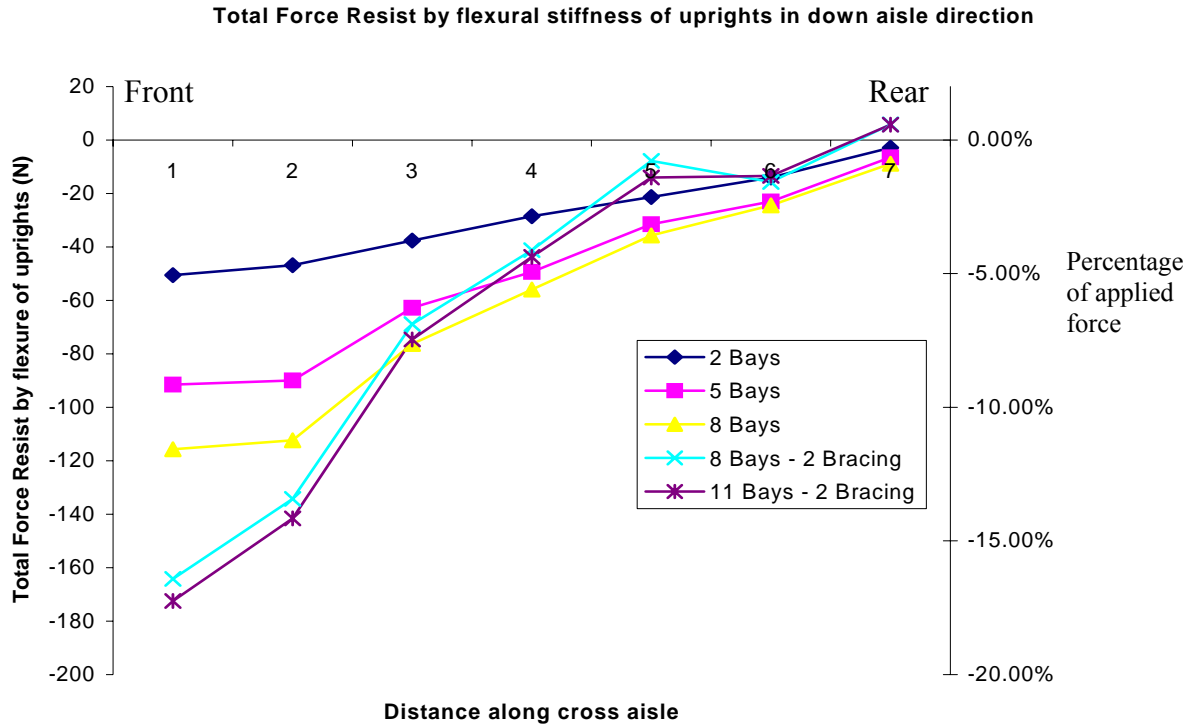


Figure 9a. Shear forces resisted by flexural stiffness of uprights (S_f)

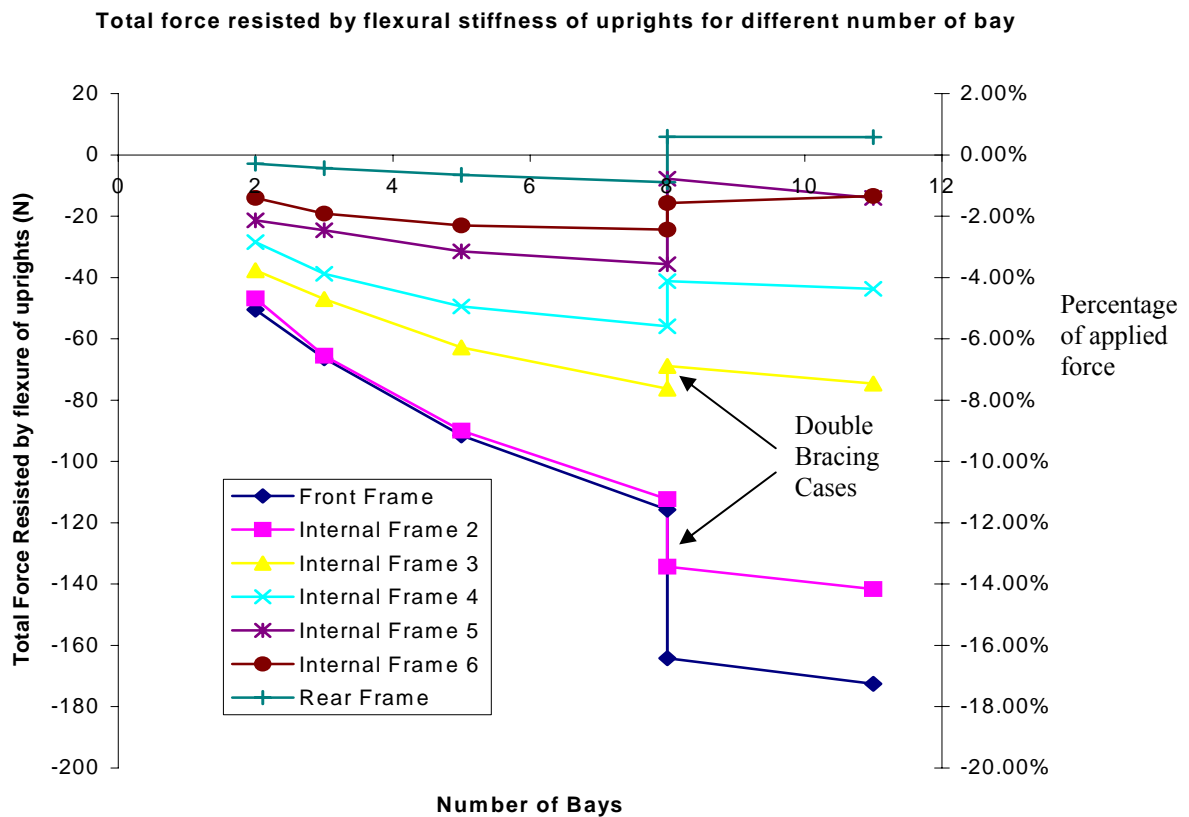


Figure 9b. Shear forces resisted by flexural stiffness of uprights (S_f)

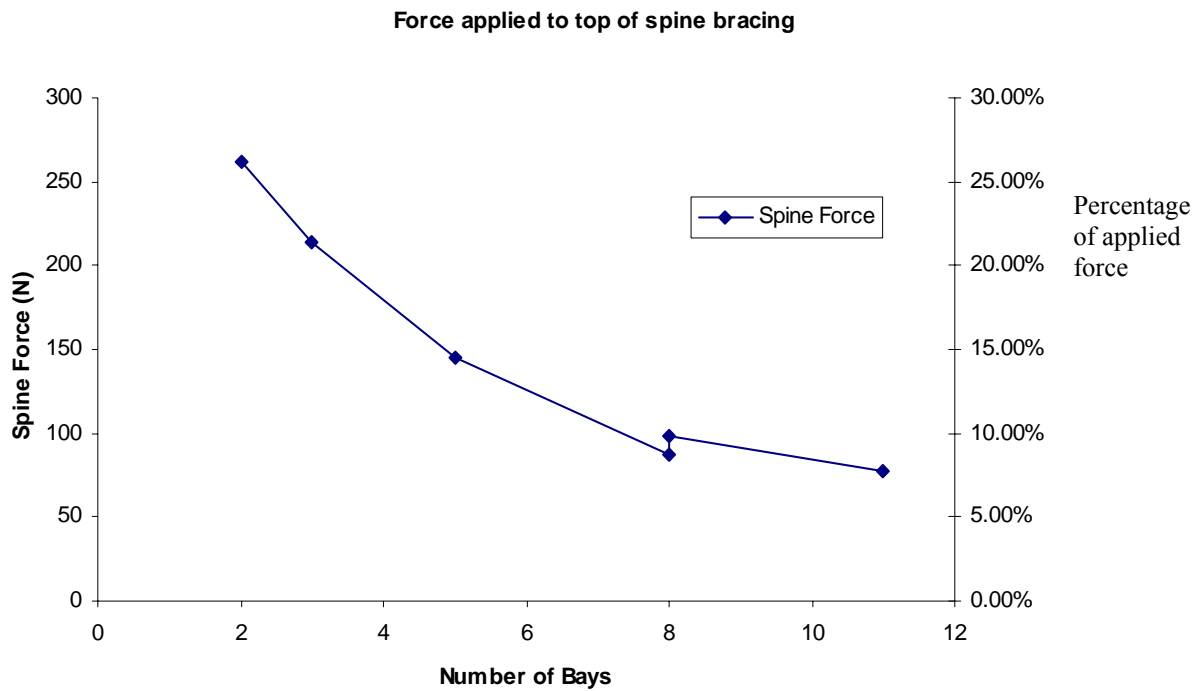


Figure 10. Horizontal force applied to top of spine bracing (S_s)

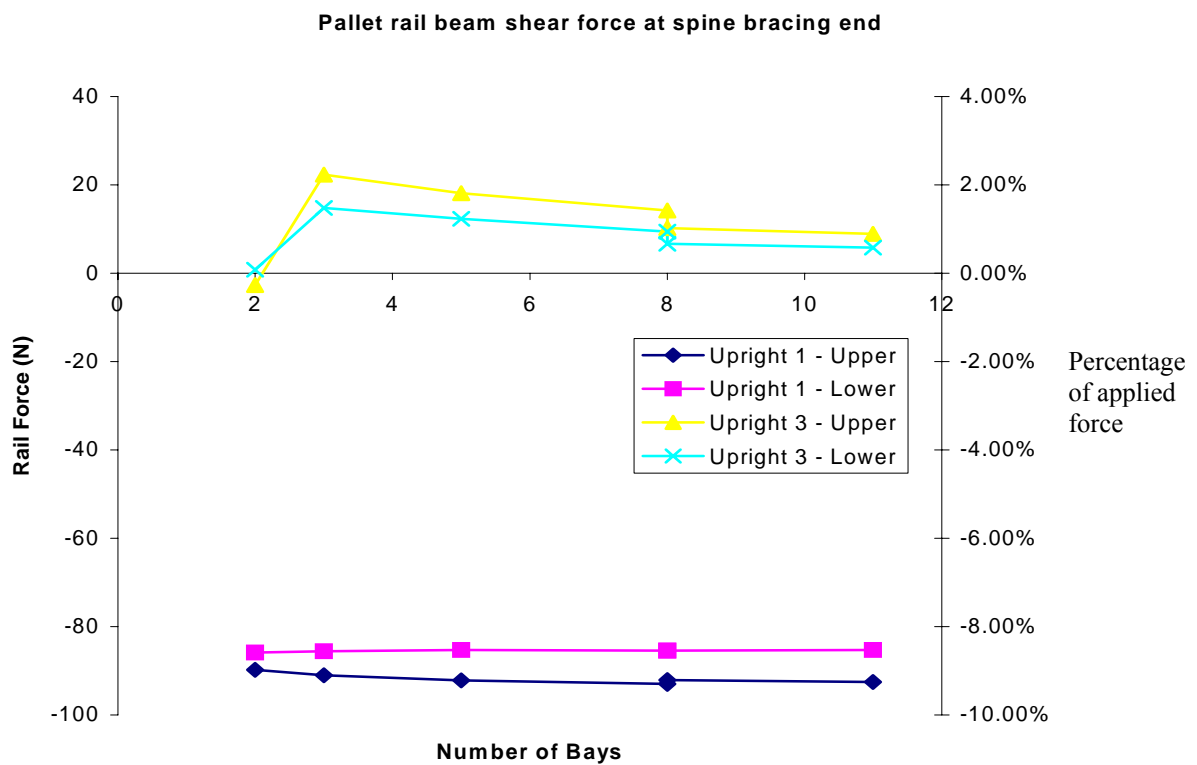


Figure 11. Pallet rail beam force to spine bracing

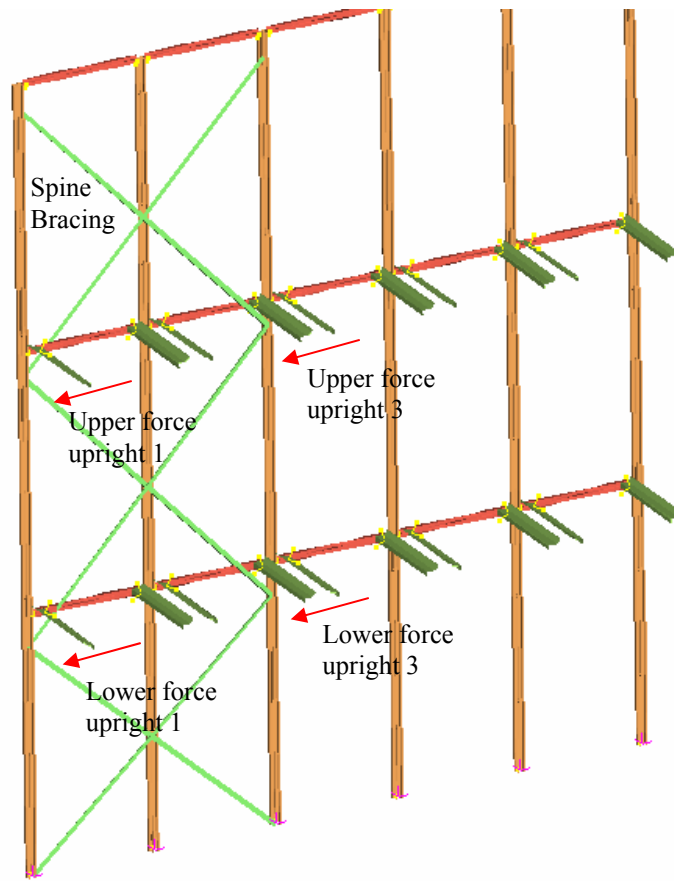


Figure 12. Pallet rail beam forces

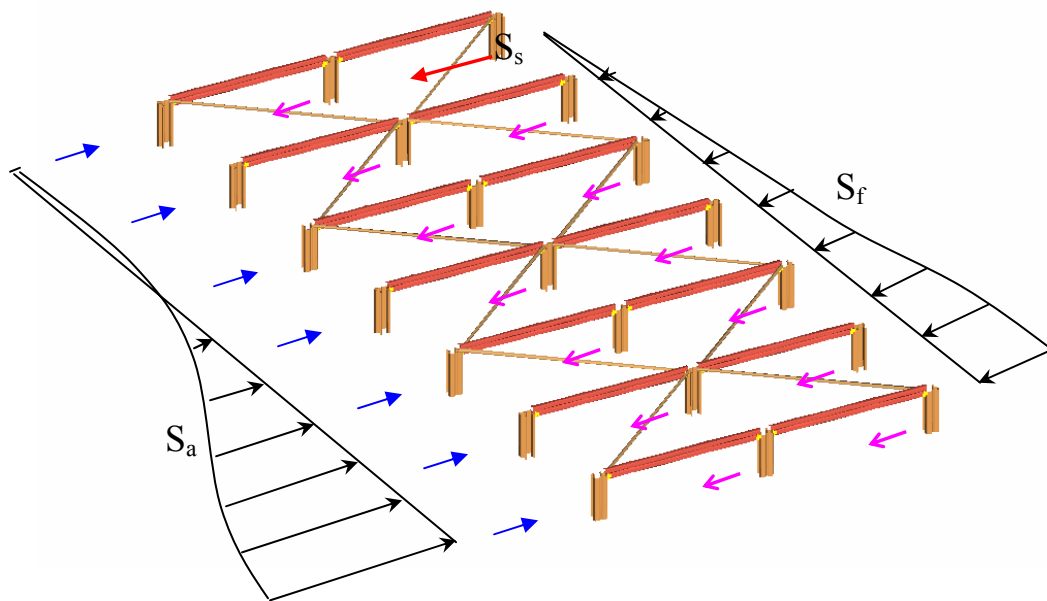


Figure 13. FBD of 2 bays plan bracing

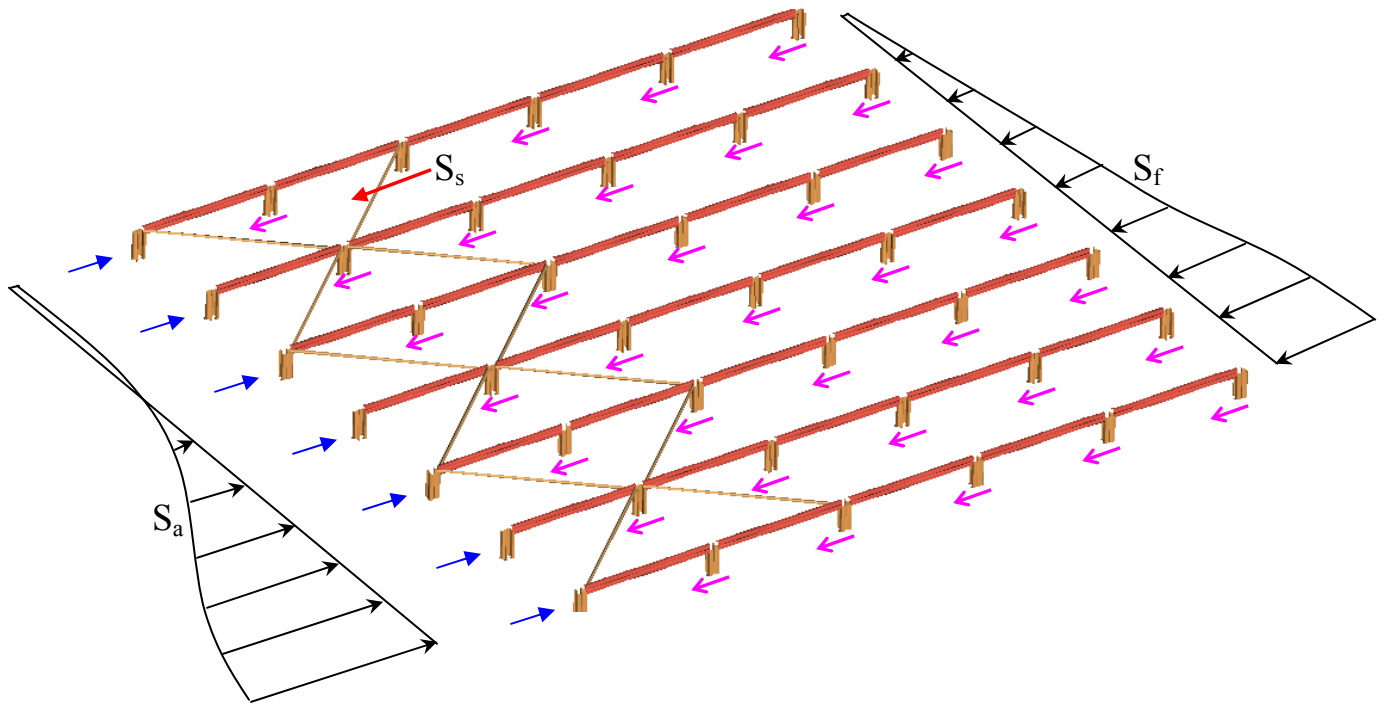


Figure 14. FBD of 5 bays plan bracing

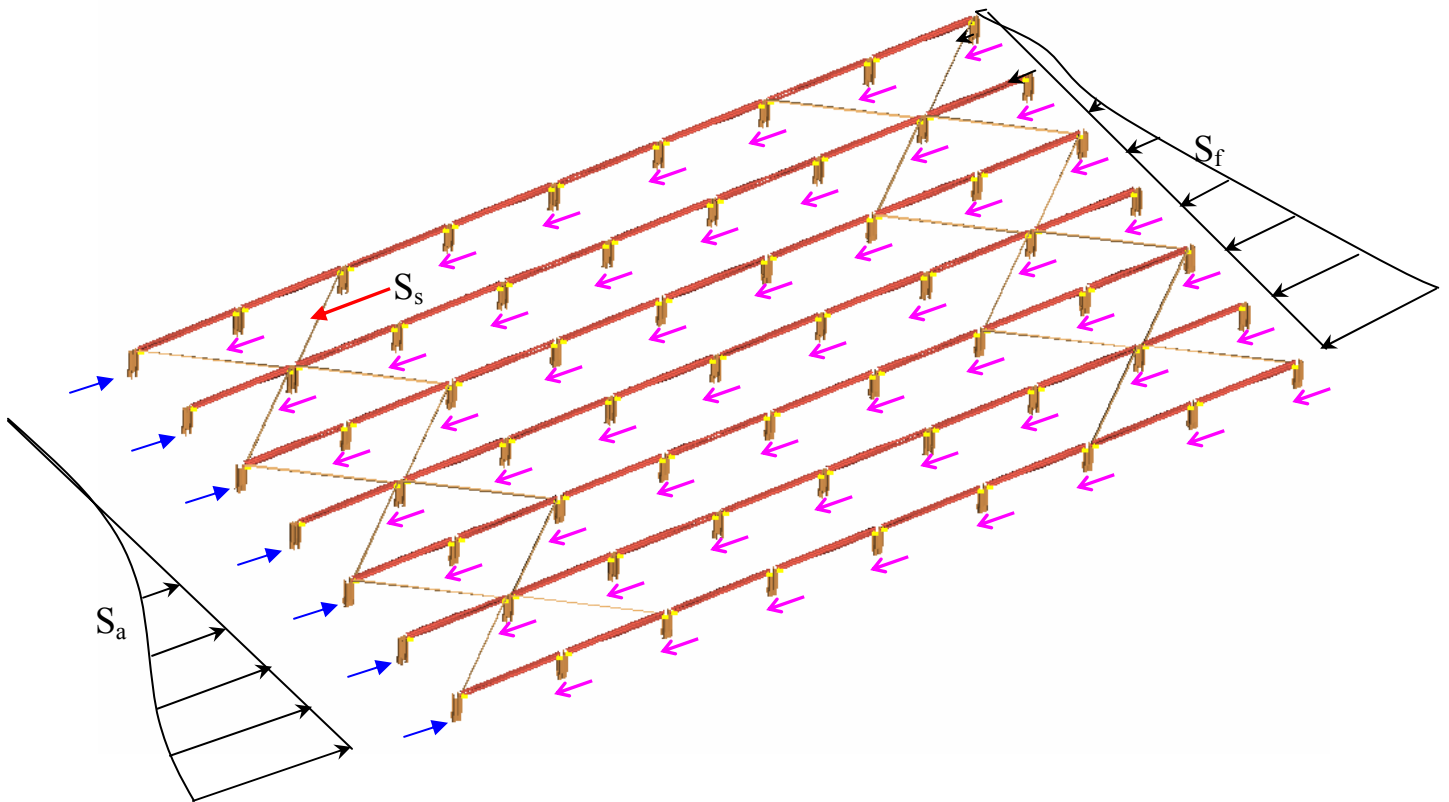


Figure 15. FBD of 8 bays plan bracing (2 bracing bays)

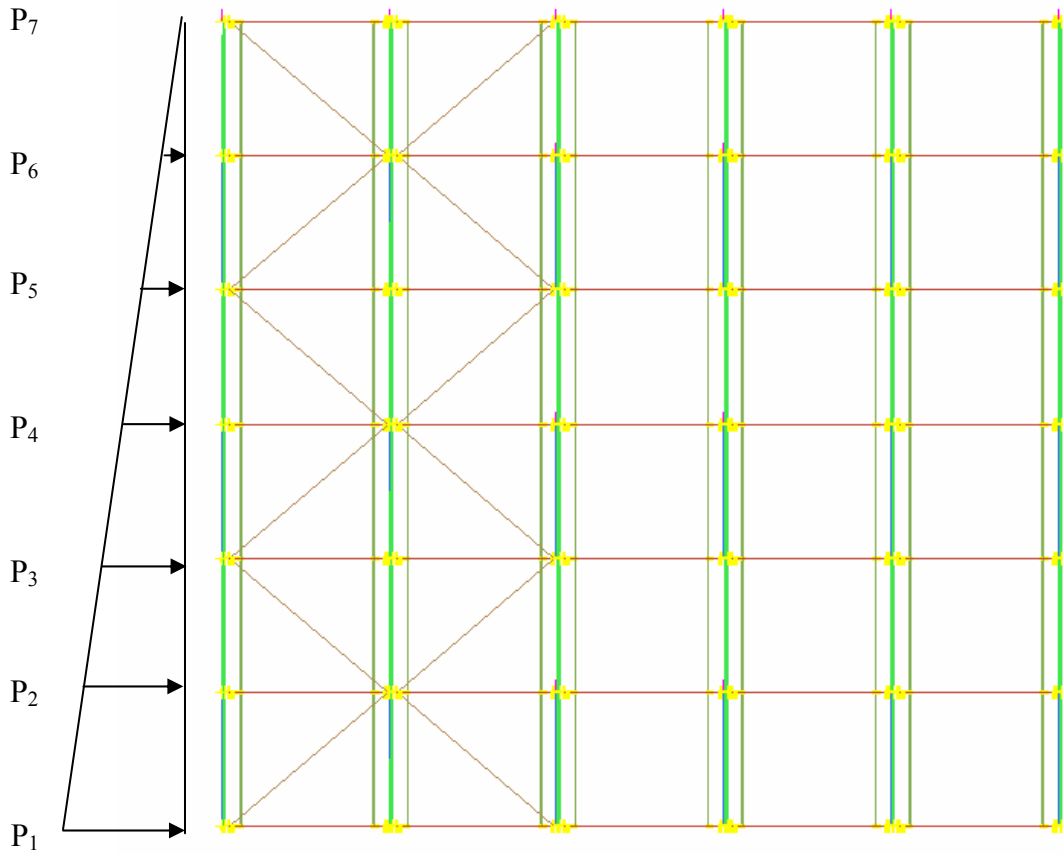


Figure 16. Forces applied to plan bracing

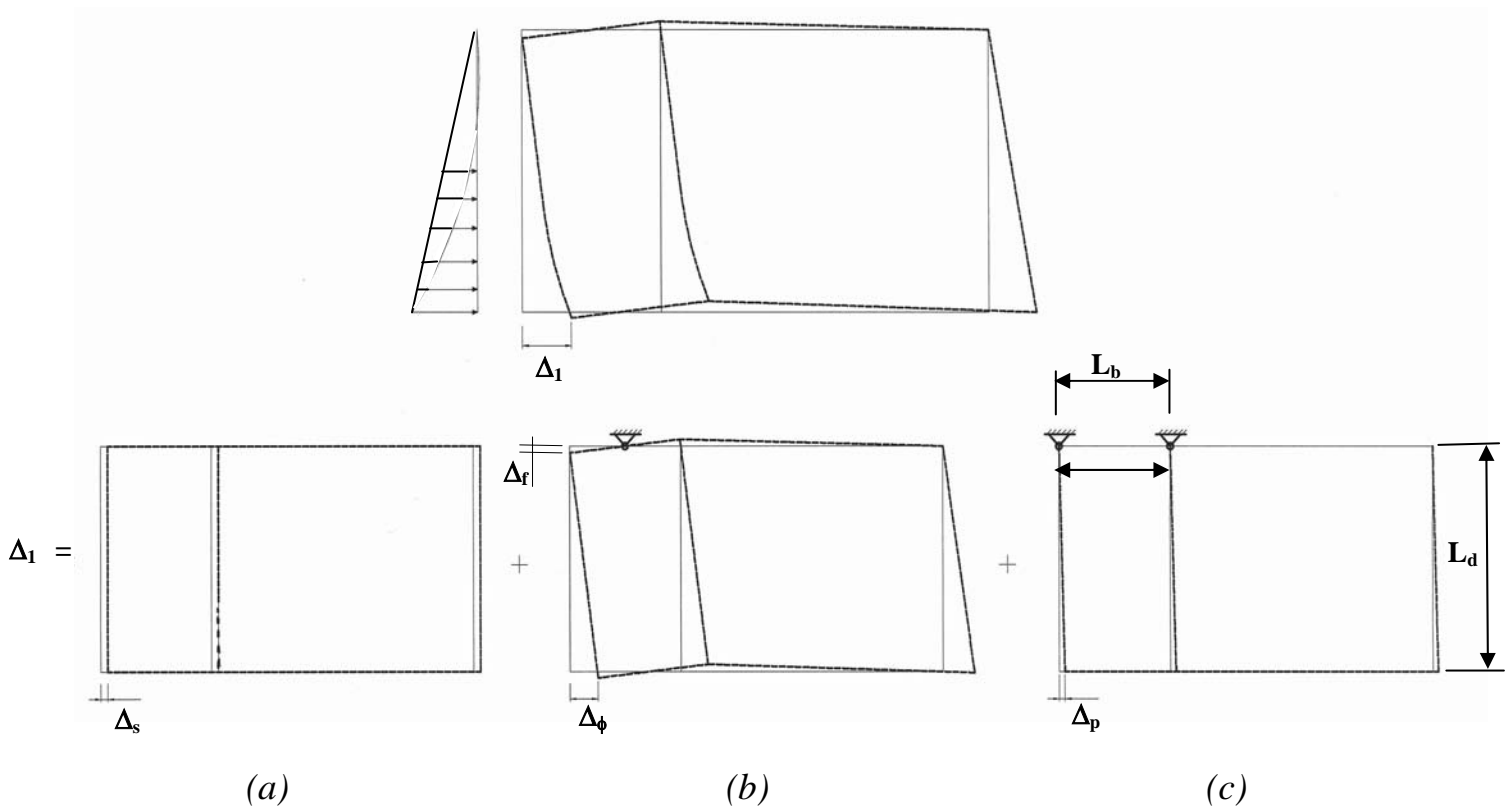


Figure 17. Deformations of top level of frame

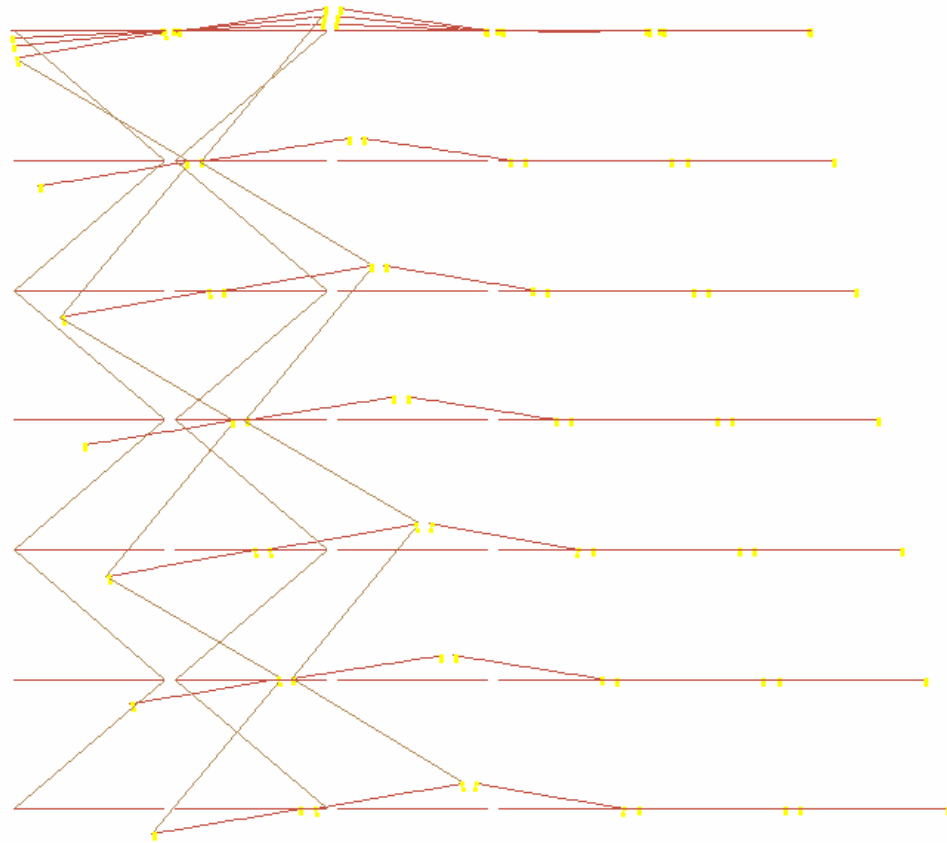


Figure 18. Deflected shape of top plan bracing